Structural effects in electrocatalysis: electrooxidation of carbon monoxide on Pt_3Sn single-crystal alloy surfaces

Hubert A. Gasteiger [1], Nenad M. Marković and Philip N. Ross Jr.

Materials Sciences Division, Lawrence Berkeley Laboratory, University of California, Berkeley, CA 94720, USA

Received 11 August 1995; accepted 15 September 1995

The kinetics of the electrochemical oxidation of carbon monoxide (CO) and CO/hydrogen mixtures (0.1 and 2% CO) in sulfuric acid electrolyte at 25–62°C was studied on different surfaces of the ordered single crystal Pt_3Sn alloy. Characterization of the surface composition and structure was determined in UHV using low energy electron diffraction (LEED), Auger electron spectroscopy (AES), and low energy ion scattering (LEIS) prior to determining the electrode kinetics using the classical rotating disk method (RDE) with CO dissolved in the electrolyte. Clean annealed and sputtered-cleaned but not-annealed surfaces of (110) and (111) orientation were studied. A remarkable difference in activity was observed between the annealed (111) surface and the sputtered but not-annealed (110) surface, with both surfaces having the same nominal surface composition, 20–25 at% Sn, but different local structures. The onset potential for CO oxidation on the (111) surface was shifted cathodically by 0.13 V relative to that for the sputtered (110) surface, and the onset comes remarkably close to 0 V on the reversible hydrogen potential scale. Relative to pure Pt surfaces (of any crystal structure), the potential shift is more than 0.5 V, corresponding to a catalytic activity that is higher by more than four orders of magnitude. Comparable shifts were observed for the oxidation of CO/H_2 mixtures. Both the structure sensitivity and the high catalytic activity of the Pt_3Sn surface are attributed to an adsorbed state of CO unique to this alloy and occurs at relatively high coverage on the (111) surface.

Keywords: electrocatalysis; carbon monoxide; platinum–tin alloy; single crystal; electrooxidation

1. Introduction

A major problem in the development of low temperature fuel cells, e.g., < 100°C, for transportation applications is the deactivation of the Pt anode electrocatalyst by even trace levels, e.g., 10–100 ppm, of carbon monoxide [1]. This deactivation necessitates either the use of pure hydrogen stored on-board the vehicle or an extensive purification system for hydrogen generated on-board by steam reforming a hydrocarbon fuel. A considerable simplification occurs in the case of methanol as the fuel if the anode catalyst will "tolerate" on the order of 1% CO, since methanol can be steam reformed in a single step to these levels [2]. In this context, "tolerate" is defined as a minimal change in anode polarization when the gas feed to the anode is switched from pure hydrogen to the reformate gas. Previously, we presented detailed studies of the electrooxidation of H_2 [3], CO [3] and their mixtures [4] on Pt, Ru and Pt–Ru alloys using UHV surface preparation and characterization combined with the classical electrochemical rotating disk electrode (RDE) technique for kinetic evaluation of the reaction rates. We showed that pure Ru is the most active surface for CO oxidation, but because it is a very inactive surface for hydrogen oxidation, a 90 at% Ru alloy surface is the most active for oxidation of H_2/CO mixtures; it should be noted that the difference in activity between pure Ru and the ~ 90 at% Ru surface for the electrooxidation of pure CO is very small, resulting in a potential shift of only ~ 0.01 V. The potential for the onset of oxidation of H_2/CO mixtures at practical rates coincides with the potential for the complete oxidative stripping of adsorbed CO (CO_{ads}), thereby freeing sites for the oxidation of hydrogen. The onset potential for the 90 at% Ru alloy is about 0.25 V lower than for pure Pt [4].

Recently, we reported [5] that a Pt_3Sn alloy surface was considerably more active than even the 90 at% Ru alloy surface for the electrooxidation of CO and/or H_2/CO mixtures. The onset potential for CO oxidation on the Pt_3Sn surface was ~ 0.15 V lower than for the Ru alloy, and the catalytic shift for H_2/CO mixtures was ~ 0.1 V. The Pt_3Sn sample we used in that study was a (110) single crystal that had been sputtered but not annealed in UHV. We report here our finding of a remarkable structure sensitivity for the electrooxidation of CO and/or H_2/CO mixtures on different surfaces of the Pt_3Sn crystal. We used two different crystal faces, (111) and (110), and two different methods of preparing the surfaces in UHV: argon ion etching to produce a clean surface having compositions close to the bulk composition, 25 at% Sn, and the annealed surfaces, which in the case of (110) is a 50 at% Sn surface. The annealed (111) surface and the sputtered (110) have nearly the same surface composition, between 20 and 25 at% Sn, but very different surface structures/geometries, providing a unique opportunity to study a purely structural effect with an alloy catalyst. As we report here, these two

[1] To whom correspondence should be addressed.

© J.C. Baltzer AG, Science Publishers

surfaces have remarkably different activities, with the onset potential for CO oxidation being lower by 0.13 V on the annealed (111) surface and actually approaching 0 V on the reversible hydrogen potential scale. We also report examples of very low overpotentials for the oxidation of H_2/CO mixtures. Since it is observed that small particles of Pt [6] and Pt alloys [7] supported on carbon black expose primarily (111) facets, these results provide a guide to what might be expected from a highly dispersed supported Pt_3Sn alloy electrocatalyst in a fuel cell anode fed with steam-reformed or cracked methanol.

The surface chemistry of Pt_3Sn single crystals has been reasonably well studied in recent years, with the clean annealed surfaces of all three index faces determined by a variety of techniques, including low energy ion scattering (LEIS) [8,9], dynamical low energy electron diffraction (LEED) [10], and element selective CO chemisorption [11]. A seminal theoretical treatment of the surface thermodynamics of Pt_3Sn was developed by Van Santen and Sachtler [12], followed by numerous experimental studies of surface composition of polycrystalline Pt–Sn alloys by Biloen and co-workers [13] which for the most part confirmed the predictions of the theory. As reported earlier in this journal [8], the compositions of the clean annealed surfaces of all three low index surfaces of Pt_3Sn are as predicted by the generalized broken bond model of Van Santen and Sachtler.

2. Experimental

The Pt_3Sn (110) and (111) oriented single crystals were the same as those used in previous UHV [8–11] and electrochemical studies [14] in this laboratory. The methodology used for studying the electrooxidation of CO was the same as that used previously for Pt–Ru alloys and most recently for $Pt_3Sn(110)$ [3–5]. Briefly summarized, the method consists of sample cleaning in UHV by ion bombardment followed by high temperature annealing, surface analysis by Auger electron spectroscopy (AES) and low energy ion scattering (LEIS), and transfer of the sample to a specially designed rotating disk electrode apparatus. Subsequently, the UHV-prepared alloy surfaces were immersed under potential control at $\sim$ 0.05 V in 0.5 M H_2SO_4 (Baker, Ultrex) and experiments were conducted without any further pretreatment (e.g., potential cycling). In the case of $Pt_3Sn(110)$, two surface states were used, one the annealed state, having the ideal composition (by LEIS) of 50 at%, and a second state created by mild sputtering of the annealed surface with 0.5 keV Ar ions ($i \approx 10$ μA/cm^2, 63° angle of incidence) resulting in a Sn surface concentration of ca. 20 at% Sn by LEIS. Details of the LEIS experimental set-up may be found in ref. [15]. Previous work [14] had established that Sn has a narrow potential window of stability in the surface, requiring that the potential not exceed 0.5 V versus the standard hydrogen electrode. Within this potential limit, no loss of Sn was observed during the course of the experiments (typically several hours). All potentials are referenced to the reversible hydrogen electrode (RHE) in the same electrolyte (0.5 M H_2SO_4) at 1 atm hydrogen (Spectra Gases, 6N). The CO/H_2 and CO/Ar gas mixtures as well as pure CO (6N H_2, 4N CO) were puchased from Matheson; the purity of the argon purge gas was 5N8 (Air Products).

3. Results and discussion

3.1. Surface composition

The AES and LEIS spectra for the three surfaces used in this study are shown in the insert in fig. 1. The composition of the clean annealed surface of the $Pt_3Sn(111)$ was established in previous studies [8–11]. The surface composition is the same as the bulk, 25 at% Sn, which is the surface structure expected for bulk termination of the crystal. We used this composition of the annealed (111) crystal to calibrate the LEIS intensities and to calculate the surface compositions of the (110) crystal from the LEIS spectra. The results, shown in fig. 1c, are that the clean annealed surface of the (110) crystal is $\sim$ 53 at% Sn, while the sputtered surface is close to the bulk composition, $\sim$ 21 at% Sn. The latter corresponds to the preferential termination of the surface in the (110) planes of the bulk $L1_2$ lattice, i.e., without exposing any of the pure Pt(220) planes. This preferential termination is consistent with thermodynamic models, e.g., ref. [12]. Thus, the sputtered (110) and the annealed (111) have essentially identical compositions but different structures, providing a unique opportunity in alloy catalysis to study a purely structural effect on the reactivity of an alloy surface.

We also show the AES spectra for all three surfaces in figs. 1a and 1b for a different purpose. From the AES Pt/Sn intensity ratios, one might conclude that the annealed (111) and (110) crystals have the same surface composition when they do not. This result serves to emphasize both the importance of ion scattering in determining true surface composition of alloys and, if AES is the only tool available, the importance of accounting for subsurface contributions to the AES spectra. The qualitative explanation for the AES ratios of the annealed (111) and (110) Pt_3Sn crystals (see the table in fig. 1), assuming both have bulk truncation structures, is that for the (110) crystal the second layer is pure Pt, while in the (111) crystal the second layer (and all deeper layers) have the same composition as the first layer. Thus, the contribution of Auger emission from the pure Pt second layer in the (110) crystal causes the Pt/Sn AES ratio to be much larger than the ratio would be with emission only from the first layer. Quantitative surface analysis of the (110) crystal with AES is quite com-

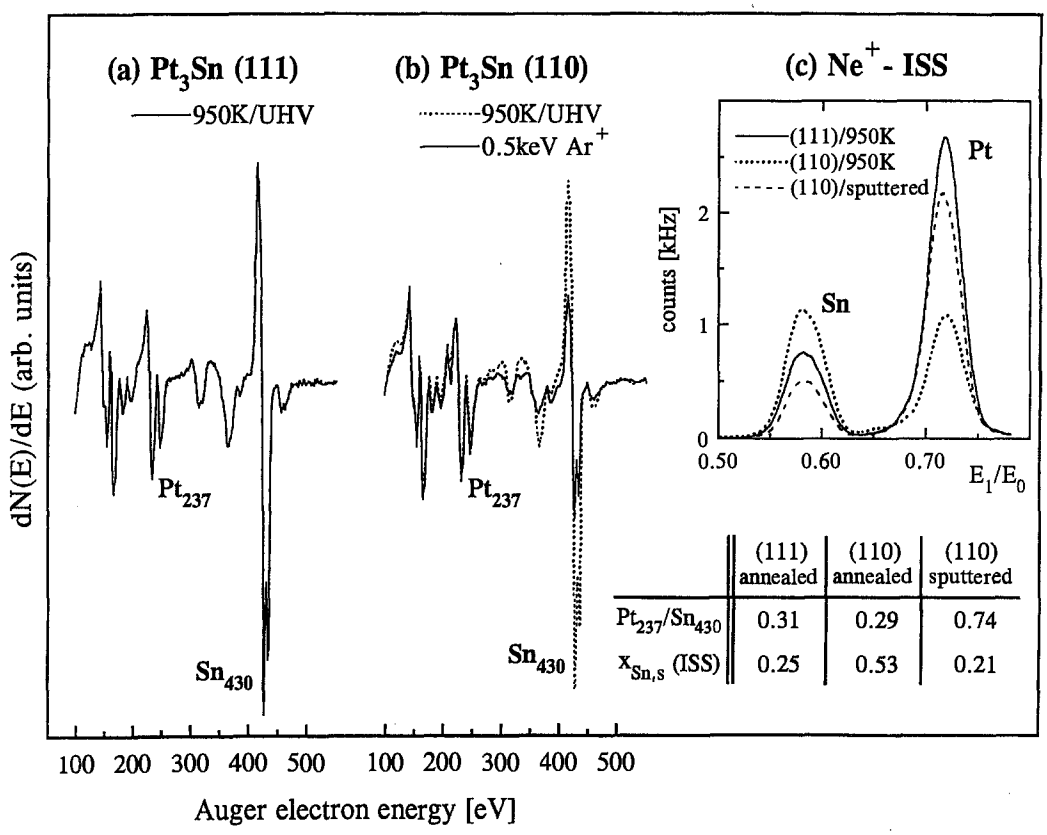

Fig. 1. Auger electron spectra (3 keV beam energy, 3 eV_{p-p} modulation, −5 μA beam current) of $Pt_3Sn(hkl)$ surfaces: (a) (111) surface after sputter-cleaning and annealing at 950 K; (b) (110) surface after sputter-cleaning with 0.5 keV Ar^+ (solid curve) and after annealing (dotted curve). (c) Low energy ion scattering (LEIS) spectra of the same three surfaces (1 keV Ne^+, 127° scattering angle, 45° incidence angle, normal take-off angle, 30 nA/cm^2 ion current density, 100 s/spectrum). The table summarizes AES ratios and surface compositions calculated from the LEIS spectra above (see text).

plicated, requiring modeling of emission from several subsurface layers with dynamical scattering of the outgoing Auger electron.

3.2. Cyclic voltammetry in 0.5 M H_2SO_4 at 25° C

The corresponding base voltammetry curves for the three surfaces, immediately following transfer from UHV in argon purged electrolyte are shown in fig. 2. The annealed (110) surface is essentially featureless in the region shown, which is primarily the hydrogen adsorption potential region. The hydrogen adsorption pseudocapacitance is considerably reduced from that of the corresponding Sn-free Pt(110) surface, as one might expect from an alloying element that does not adsorb hydrogen. The (111) alloy surface also has a decrease in the hydrogen adsorption pseudocapacitance (at 0–0.3 V) relative to the Sn-free surface, but, on the other hand, the voltammetry is not featureless, and has a reversible redox feature at a potential where there is none on the Sn-free Pt(111) surface, at ca. 0.35 V. Similar voltammetry for $Pt_3Sn(111)$ in both sulfuric and hydrofluoric acid was presented in an earlier study [14]. We did not know then, nor do we know now, what this prominent feature at ca. 0.35 V is; we can only say that it is highly reversible, i.e., there is no shift in peak potential with sweep rate up to 1 V/s. It could be any number of processes, hydrogen adsorption, anion adsorption, OH adsorption, or a Sn surface redox process. In the following, however, it will become clear that the onset potential for CO oxidation is significantly negative of this feature, such that it does not seem to have any relation to the properties of the surface for the electrooxidation of CO.

3.3. CO electrooxidation at 25° C

In order to study the activity of fully poisoned surfaces toward the oxidation of CO and CO/H_2 mixtures (simulating the conditions encountered in a fuel cell), the electrode potential was held at the immersion potential (~ 0.05 V) for 3 min at rotation rate of 2500 rpm while purging the electrolyte with the respective gas. The polarization curves for CO electrooxidation at ambient temperature and 2500 rpm, under conditions of a slow (1 mV/s) potential sweep originating from ~ 0.05 V, are shown in fig. 3. We have demonstrated previously [4] that the polarization for CO oxidation under these slow sweeping conditions is essentially the same as the steady-state polarization. Consequently, in the entire potential range chosen for these experiments, the hysteresis in the

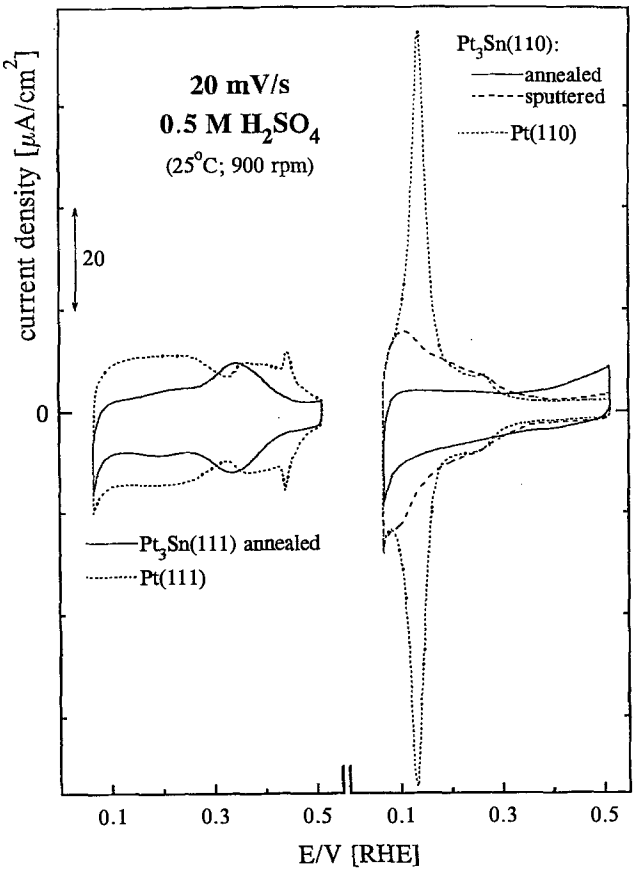

Fig. 2. Cyclic voltammetry of the three Pt_3Sn surfaces of fig. 1 compared to the voltammetry of the pure Pt surface of the same crystal structure. Both the UHV-prepared alloy electrodes and the flame-annealed Pt single crystals were mounted in a RDE arbor and immersed under potential control at ~ 0.05 V; no other pre-treatment was applied. 20 mV/s, 900 rpm, 25°C, 0.5 M H_2SO_4.

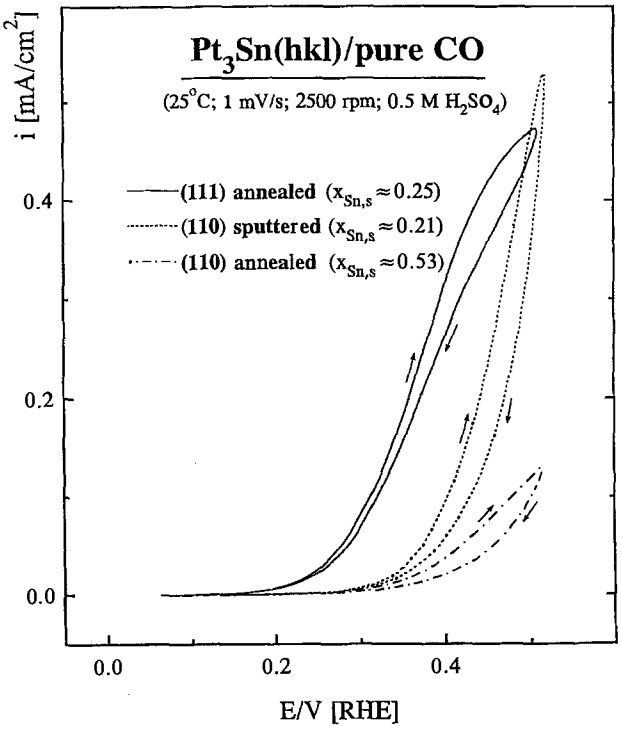

Fig. 3. Current–potential curves for the electrooxidation of CO gas (1 atm) dissolved in 0.5 M H_2SO_4 at 25°C on the three UHV-prepared electrode surfaces of fig. 1. Prior to the positive-going sweep, the electrode potential was held at ~ 0.05 V for 3 min to ensure the complete poisoning of the surfaces with dissolved CO. 1 mV/s, 2500 rpm.

current between the positive and negative going sweeps is rather small, on the order of 0.02 V.

At the rotation rate of 2500 rpm the diffusion limited CO oxidation current density at 25°C is ~ 2.3 mA/cm² [3], implying that the current densities measured in the potential range displayed in fig. 3 are essentially kinetically controlled and do not contain any significant mass transport resistances. The onset potential for CO oxidation on the (111) surface is ~ 0.1 V lower than for the sputtered (110) surface having (nearly) the same Sn surface concentration, demonstrating an unusually large structural effect. Whereas the activity of the sputtered (110) surface is comparable to the measurements by Motoo et al. [16] on Pt–Sn clusters, the Pt_3Sn(111) surface exhibits the highest CO oxidation activity ever measured in this laboratory and ever reported in the literature, with an overpotential reduced by ~ 0.25 and ~ 0.55 V if compared to pure Ru and pure Pt, respectively [3] (an interesting parallel to this outstanding activity of Pt–Sn electrodes may be found in the gas phase oxidation of CO at room temperature on Pt supported on SnO_2 mainly used in closed cycle CO_2 lasers [17,18]). The potential shift between the annealed (111) and the sputtered (110) surfaces corresponds to a difference in catalytic activity of more than an order of magnitude in the low potential region (i.e., in the vicinity of 0.2 V), which is the region of greatest practical relevance. If one assumes that the CO oxidation mechanism on Pt–Sn electrodes proceeds through a Langmuir–Hinshelwood type reaction, where CO is adsorbed exclusively on Pt sites and oxygen-containing species (OH_{ads}) are nucleated on Sn atoms, the maximum activity would be expected at a Sn surface composition of ~ 50 at%. On the contrary, however, the annealed Pt_3Sn(110) surface ($x_{Sn,s} \approx 0.5$) exhibits the highest overpotential for CO oxidation of the electrodes studied in fig. 3, the cause of which will be discussed in section 3.5.

3.4. CO and CO/H_2 electrooxidation at 62°C

The prime incentive to assess the electrooxidation rates of CO and CO/H_2 mixtures at 62°C is the envisaged technological use of a Pt–Sn alloy catalyst as an anode electrode in a polymer electrolyte membrane (PEM) fuel cell [1] with reformed methanol as the fuel. The resulting CO concentrations in the hydrogen feed stream are 2% in a steam reforming process or up to 18% in a partial oxidation reformer with its superior load-following characteristics [19]; significantly lower CO contamination (0.1–0.01%) from methanol-derived hydrogen gas can only be achieved if the above processes

are followed by a water gas shift reactor and a selective oxidizer [20].

Based on section 3.3 and on the extremely high activity of all three Pt_3Sn surfaces toward the electrooxidation of hydrogen at 62°C, viz., on the order of 0.1 A/cm^2 [5], the most promising candidates for the oxidation of pure CO and CO/H_2 mixtures at elevated temperature are both the annealed (111) and the sputtered (110) surfaces. Their potentiodynamic (1 mV/s) activity toward the oxidation of pure CO, 2% CO/H_2, and 0.1% CO/H_2 at 2500 rpm and 62°C in 0.5 M H_2SO_4 is shown in fig. 4; only the positive-going sweeps are shown since the hysteresis between positive- and negative-going sweeps is negligibly small (0.01–0.02 V). Under these conditions, the diffusion limited oxidation current densities for pure CO and pure H_2 are 2.33 and 4.04 mA/cm^2, respectively [4], such that mass transport resistances are negligible below ~ 0.5 mA/cm^2. Similar to the room temperature data (fig. 3), the overpotential for CO oxidation on the (111) surface is ~ 0.13 V lower than on the sputtered (110) surface with (nearly) the same Sn surface composition, with an onset of the CO oxidation reaction at ~ 0.15 V on the more active electrode.

As the CO concentration is being reduced to 2% CO/H_2, the activity of the (111) surface decreases slightly, fig. 4a, indicating the preferential oxidation of CO versus hydrogen; only if the CO concentration reaches a level of 1000 ppm, the oxidation currents exceed the values for pure CO. On the contrary, the sputtered (110) surface which is less active for pure CO, fig. 4b, displays a significant decrease in the overpotential for CO/H_2 oxidation as the CO concentration is being reduced; nevertheless, for all gases, the sputtered (110) surface is always less active than the annealed (111) surface. For analogous experiments with various Pt–Ru alloy electrodes, a negative reaction order with

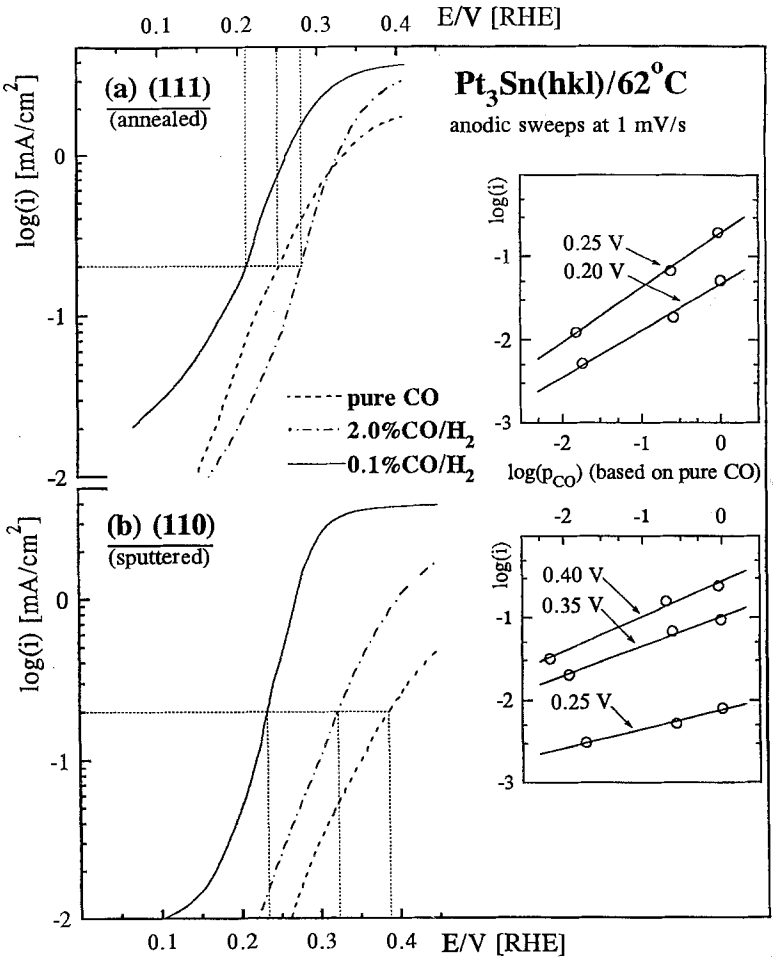

Fig. 4. Positive-going potentiodynamic (1 mV/s) oxidation current densities for pure CO, 2% CO/H_2, and 0.1% CO/H_2 on UHV-prepared $Pt_3Sn(hkl)$ rotating disk electrodes (2500 rpm) at 62°C: (a) annealed (111) surface with $x_{Sn,s} \approx 0.25$; (b) sputtered (0.5 keV Ar^+) (110) surface with $x_{Sn,s} \approx 0.21$. Prior to the positive-going sweep, the electrode potential was held at ~ 0.05 V for 3 min to ensure the complete poisoning of the surfaces with dissolved CO. The dotted line indicates the potentials at which a current density of 0.2 mA/cm^2 is reached (this potential under identical conditions on pure Pt [4] corresponds to ~ 0.8 V, ~ 0.68 V and ~ 0.5 V for pure CO, 2% CO/H_2, and 0.1% CO/H_2, respectively). Inserts: Logarithmic reaction order plots of current density versus CO partial pressure (p_{CO}) at the indicated electrode potentials; p_{CO} is based on the saturation pressure of pure CO under reaction conditions. Data were extracted from experiments with pure CO, 26% CO/Ar, and 2% CO/Ar (for details see ref. [4]).

respect to CO was observed [4], effecting largely diminished overpotentials for CO/H_2 oxidation compared to the oxidation of pure CO. This is in contrast to the data shown in fig. 4: based on the diffusion limited CO oxidation current density of ~ 0.047 mA/cm^2 for 2% CO/H_2 [4], a zero reaction order, m, with respect to CO partial pressure, p_{CO}, (i.e., $i = kp_{CO}^m$) would imply that CO would be depleted from the diffusion layer at a potential of ~ 0.20 V and 0.32 V on the (111) and (110) surfaces, respectively, such that essentially diffusion limited hydrogen oxidation current densities (~ 4 mA/cm^2) would have to be measured at these potentials. Quite clearly, this is not the case, and, indeed, measurements with CO/Ar gas mixtures did establish positive reaction orders with respect to CO (see inserts of fig. 4), with values ranging from $m = 0.55$–0.65 for the (111) and $m = 0.25$–0.45 for the (110) surface, the mechanistic ramifications of which will be discussed in section 3.5.

At last we will compare the activity of direct methanol oxidation with the oxidation of CO/H_2 mixtures. The most active electrocatalyst for direct methanol oxidation at 60°C in the same electrolyte is a Pt–Ru electrode with a Ru surface composition of ~ 30 at%, yielding a current density of 0.2 mA/cm^2 at 0.4 V [21]. The dotted lines in fig. 4 indicate the potentials at which this current density is attained on Pt_3Sn electrodes with different CO/H_2 mixtures. On the (111) surface, pure CO can be oxidized at a 0.15 V lower overpotential (i.e., at 0.25 V), such that $Pt_3Sn(111)$ would be of particular technological interest for the oxidation of H_2/CO mixtures containing a high percentage of CO, e.g., 33% CO produced by thermal cracking of methanol or ~ 18% CO produced by partial oxidation [19]. The polarization curve for cracked methanol would be close to the curve for pure CO in fig. 4a and would present a gain in overpotential of ~ 0.15 V compared to the direct electrooxidation of methanol on Pt–Ru electrocatalysts [21]. This gain in voltage more than compensates for the energy required to crack methanol [22] and there are additional benefits to cracked methanol as a PEM fuel cell feedstock versus pure methanol, the most obvious being the elimination of the problem of "crossover" of methanol to the cathode due to the high solubility of methanol in the membrane [23].

3.5. CO oxidation mechanism on Pt–Sn electrodes

As we will discuss in detail elsewhere [24], the mechanism of CO electrooxidation on Pt–Sn alloys appears to be different from that on Pt–Ru alloy surfaces. One of the manifestations of that difference is the reaction order in CO partial pressure. On pure Pt and on all Pt–Ru surfaces the reaction order is negative, i.e., the kinetic current at a fixed potential actually decreases with increasing CO partial pressure, an effect deriving from the competition between CO adsorption and OH_{ads} nucleation [4]. For this reason, the resulting low surface concentration of OH_{ads} limits the rate of the bimolecular Langmuir–Hinshelwood type reaction between CO_{ads} and OH_{ads} on Pt–Ru surfaces if CO is supplied continuously to the electrode surface, which is the case in both RDE experiments and under actual fuel cell conditions. In contrast, the lack of CO adsorption on Sn surface atoms, inferred from UHV experiments [11], prevents the interference of CO with the process of OH_{ads} formation on Sn, effecting a positive reaction order with respect to CO (see inserts of fig. 4). Evidence for the formation of oxygen-containing species on Sn sites may be inferred from studies on the gas phase oxidation of CO on Pt/SnO_x [18,25] (it will be discussed in more detail in our full paper [24]). Quite clearly, this correlation of catalytic activity to reaction order is one of the keys to the reaction mechanism. It is beyond the scope of this communication to discuss the mechanism in detail, and the evidence supporting it, but it is useful to invoke here the central elements of the proposed mechanism to explain the remarkable structure sensitivity of CO electrooxidation on Pt–Sn surfaces.

Besides the remarkable difference in the reaction order with respect to solution phase CO observed between Pt–Ru and Pt–Sn, the other striking distinction between these two catalyst systems is the fact that complete oxidative stripping of CO adsorbed on Pt–Ru occurs at potentials as low as 0.4 V [26, 27], but only a small fraction (~ 0.3 ML) of CO adsorbed on Pt-Sn can be stripped in the potential range below 0.5 V, in spite of its far superior activity toward the continuous oxidation of solution phase CO [27]. While the physical origin of this behavior will be discussed in our full paper [24], the experimental evidence implies that *only* weakly bonded CO can be oxidized in a Langmuir–Hinshelwood type reaction on Pt–Sn surfaces. The effect of a weakly bonded state of CO on the Langmuir–Hinshelwood oxidation of CO_{ads} on Pt–Sn may be thought analogous to the same oxidation mechanism of CO_{ads} and adsorbed oxygen on Pt(111) which was first outlined by Campbell et al. [28]. They demonstrated that the activation energy for this surface reaction is reduced dramatically (by a factor of two) if the CO coverage is high, an observation which they ascribed to the largely reduced CO adsorption energy at high CO coverage (i.e., weakly adsorbed CO) due to repulsive CO–CO interaction [29]. A similar conclusion was reached by Anderson et al. [30] in molecular orbital calculations, which indicated that the activation energy for the reaction between OH_{ads} and CO_{ads} on a Pt surface is decreased if the coverage of the reactants is high, i.e., if their adsorption energy is reduced. Therefore, in general terms, weakly adsorbed CO refers to CO in its high coverage state in which it is rendered more active towards its oxidation.

We have demonstrated before in CO_{ads} thermal desorption spectra [11], that as much as 30% of the CO on $Pt_3Sn(111)$ is in the weakly adsorbed state, which is only populated either at low temperature (< 250 K) or at rela-

tively high CO pressure. Ross [31] has proposed that the weakly adsorbed state of CO on Pt_3Sn is a consequence of the strong intermetallic bonding in this alloy. A relatively high pressure of CO is needed to populate the weakly adsorbed state, largely effecting the observed positive reaction order with respect to solution phase CO on the $Pt_3Sn(111)$ surface.

It is possible to rationalize the structure sensitivity of the CO electrooxidation reaction on the Pt_3Sn surfaces in terms of the proposed mechanism. By inference, the population of the weakly adsorbed state requires "crowding" of the surface with adsorbed CO in order to reduce its adsorption energy via CO–CO repulsion. Since CO only adsorbs on the Pt sites of Pt–Sn alloys [11], this means crowding of the Pt sites on the surface with CO_{ads}. As Weaver and co-workers [32] first demonstrated, the unreconstructed Pt(110)-(1 × 1) surface, which is the structure of the surface in electrolyte at all potentials [33] even if one starts with a reconstructed surface ex situ, selectively adsorbs CO only on the top-row atoms, since the CO molecule is too large to sit in the "troughs". On this surface, the separation between adsorbed CO molecules at any coverage is significantly larger than on the Pt(111) surface, and the saturation coverage of CO on the unreconstructed Pt(110) face is essentially limited by the number of surface sites (0.92×10^{15} atoms/cm^2) yielding a saturation coverage of $\sim$ 1 ML in contrast to the smaller saturation coverage on Pt(111) of $\sim$ 0.6 ML presumably produced by CO–CO repulsion on the densely packed (111) plane (1.5×10^{15} atoms/cm^2) [32,34]. As a consequence, the adsorption energy of CO particularly at high θ_{CO} is larger on Pt(111) [29] than it is on Pt(110) [35] or, in other words, CO is more strongly bound on Pt(110) than on Pt(111).

In the annealed $Pt_3Sn(110)$ surface, which has the Pt(110)-(1 × 1) structure where every other row atom is Sn [8], CO_{ads} molecules are isolated from one another even when there is a CO/Pt coverage of 1, and there is no weakly bonded state created by the repulsive interaction of CO_{ads} on neighboring Pt sites. As can be seen from fig. 3, this surface is the least active for the oxidation of CO. The sputtered surface has half of the Sn atoms removed from the surface, producing additional Pt sites which increase the possibility of creating weakly bonded states of CO at high coverage, thereby enhancing the CO oxidation reaction (fig. 3). On the other hand, $Pt_3Sn(111)$ has three-fold (C_{3v}) ensembles of Pt sites interspersed with isolated Sn atoms, hence at high coverage there is crowding of CO_{ads} on neighboring sites, populating a weakly adsorbed state. Correspondingly, thermal desorption spectroscopy [11] has shown that of the three low index surfaces only the $Pt_3Sn(111)$ surface has a high fraction (ca. 30%) of the CO in the weakly bonded state, i.e., it desorbs below 300 K in UHV. Hence, the kinetics of the rds are uniquely accelerated by the relatively high population of the weakly bonded state of CO_{ads} on this surface (fig. 3) which, however, requires a high CO pressure such that the reaction order of the (111) surface is significantly larger than for the sputtered (110) surface (fig. 4).

Acknowledgement

The authors are greatly indebted to the invaluable assistance of Lee Johnson who oriented, cut, and polished the crystals used in this study. Furthermore, he and Frank Zucca were ensuring that the rotator kept rotating, not a small task for which we would like to express our thanks. This work was supported by the Assistant Secretary for Conservation and Renewable Energy, Office of Transportation Technologies, Electric and Hybrid Propulsion Division of the US Department of Energy under Contract DE-AC03-76SF00098.

References

[1] H. Tobias, M.T. Paffett, P.A. Pappin, J. Valerio and S. Gottesfeld, in: *Proc. Workshop on Direct Methanol–Air Fuel Cells*, eds. A.R. Landgrebe, R.K. Sen and D.J. Wheeler, The Electrochemical Society, Pennington (1992) Vol. 92-14, p. 37.

[2] H.S. Murray, in: *Fuel Cell*, 1985 Fuel Cell Seminar, Book of Abstracts, sponsored by the National Fuel Cell Coordinating Group, Tucson, Arizona, May 1985, p. 129.

[3] H.A. Gasteiger, N.M. Marković and P.N. Ross Jr., J. Phys. Chem. 99 (1995) 8290.

[4] H.A. Gasteiger, N.M. Marković and P.N. Ross Jr., J. Phys. Chem., in press.

[5] H.A. Gasteiger, N.M. Marković and P.N. Ross Jr., J. Phys. Chem. 99 (1995) 8945.

[6] M.L. Sattler and P.N Ross Jr., Ultramicroscopy 20 (1986) 21.

[7] V. Radmilović, H.A. Gasteiger and P.N. Ross Jr., J. Catal. 154 (1995) 98.

[8] A.N. Haner, P.N. Ross Jr. and U. Bardi, Catal. Lett. 8 (1991) 1.

[9] A.N. Haner, P.N. Ross Jr. and U. Bardi, Surf. Sci. 249 (1991) 15.

[10] A. Atrei, U. Bardi, G. Rovida, M. Torrini, E. Zanazzi and P.N. Ross Jr., Phys. Rev. B 46 (1992) 1649.

[11] A. Haner, P.N. Ross Jr., U. Bardi and A. Atrei, J. Vac. Sci. Technol. A 10 (1992) 2718.

[12] R.A. van Santen and W.M.H. Sachtler, J. Catal. 33 (1974) 202.

[13] P. Biloen, R. Bouwman, R.A. van Santen and H. Brongersma, Appl. Surf. Sci. 2 (1979) 532, and references therein.

[14] A. Haner and P.N. Ross Jr., J. Phys. Chem. 95 (1991) 3740.

[15] H.A. Gasteiger, P.N. Ross Jr. and E.J. Cairns, Surf. Sci. 293 (1993) 67.

[16] S. Motoo and M. Watanabe, J. Electroanal. Chem. 69 (1976) 429.

[17] S.D. Gardner, G.B. Hoflund, B.T. Upchurch, D.R. Schryer, E.J. Kielin and J. Schryer, J. Catal. 129 (1991) 114.

[18] A. Boulahouache, G. Kons, H.-G. Lintz and P. Schulz, Appl. Catal. A 91 (1992) 115.

[19] R. Kumar and S. Ahmed, in: *Proc. First Int. Symp. on New Materials for Fuel Cell Systems*, eds. O. Savadogo, P.R. Roberge and T.N. Veziroglu, École Polytechnique de Montréal, Montreal, (1995) pp. 224–238.

[20] S. Gottesfeld and J. Pafford, J. Electrochem. Soc. 135 (1988) 2651.

[21] H.A. Gasteiger, N. Marković, P.N. Ross Jr. and E.J. Cairns, J. Electrochem. Soc. 141 (1994) 1795.
[22] P.N. Ross Jr., J. Power Sources, submitted.
[23] D.L. Maricle and B.L. Murach, Extended Abstracts, Electrochemical Society Spring Meeting, Reno, May 1995, Vol. 95-1, pp. 736–737.
[24] H.A. Gasteiger, N.M. Marković and P.N. Ross Jr., in preparation.
[25] D.R. Schryer, B.T. Upchurch, B.D. Sidney, K.G. Brown, G.B. Hoflund and R.K. Herz, J. Catal. 130 (1991) 314.
[26] H.A. Gasteiger, N. Marković, P.N. Ross Jr. and E.J. Cairns, Electrochim. Acta 39 (1994) 1825.
[27] K. Wang, H.A. Gasteiger, N.M. Marković and P.N. Ross Jr., in preparation.
[28] C.T. Campbell, G. Ertl, H. Kuipers and J. Segner, J. Chem. Phys. 73 (1980) 5862.
[29] G. Ertl, N. Neumann and K.M. Streit, Surf. Sci. 64 (1977) 393.
[30] A.B. Anderson and E. Grantscharova, J. Phys. Chem. 99 (1995) 9143.
[31] P.N. Ross Jr., J. Vac. Sci. Technol. A 10 (1992) 2546.
[32] M.J. Weaver, S.-C. Chang, L.-W.H. Leung, X. Jiang, M. Rubel, M. Szklarczyk, D. Zurawski and A. Wieckowski, J. Electroanal. Chem. 327 (1992) 247.
[33] This laboratory, unpublished results.
[34] P.R. Norton, J.A. Davies and T.E. Jackman, Surf. Sci. 122 (1982) L593.
[35] T.E. Jackman, J.A. Davies, D.P. Jackson, W.N. Unertl and P.R. Norton, Surf. Sci. 120 (1980) 389.